Effect of Mesophase Order and Molecular Weight on the Dynamics of Nematic and Smectic Side-Group Liquid-Crystalline Polymers

Susan F. Rubin, Rangaramanujam M. Kannan, and Julia A. Kornfield*

Division of Chemistry and Chemical Engineering, California Institute of Technology, Pasadena, California 91125

Christine Boeffel

Max-Planck-Institut für Polymerforschung, Postfach 3148, D-55021 Mainz, Germany

Received July 22, 1994; Revised Manuscript Received November 28, 1994[⊗]

ABSTRACT: The dynamic moduli of side-group liquid-crystalline polymers (SG-LCPs) having methacrylate backbone, hexamethylene spacer, and phenyl benzoate mesogens are characterized as a function of molecular weight in the isotropic, nematic, and smectic phases. Molar mass was varied from 3×10^5 to 3×10^6 g/mol, corresponding to the range where the onset of entanglement is observed in the isotropic phase (approximately $1-10M_{e,iso}$). Nematic order produces a profound change in the dynamics of the entangled SG-LPCs relative to the isotropic phase; however, this effect is absent in the unentangled SG-LCPs. Oscillatory shear with large amplitude ($\gamma_0 \geq 40\%$) is effective in inducing macroscopic alignment in the nematic phase for all the SG-LCPs studied. Smectic order increases the elastic character of the fluid, but its incremental effect in a system that is entangled is relatively small. Large-amplitude shearing can be used to alter the microstructure in the smectic liquid: shearing the smectic phase produces a decrease in modulus, whereas shearing in the nematic phase followed by cooling into the smectic phase produces an increase in modulus.

Introduction

Side-group liquid-crystalline polymers (SG-LCPs) consist of a flexible polymeric backbone to which rigid, anisotropic chemical groups, termed mesogens, are attached via flexible spacers. SG-LCPs show promise in a variety of applications,[1] such as nonlinear optical materials, optical data storage media, and stress sensors. Most of the research on SG-LCPs to date has been devoted to their chemistry, particularly the effect of molecular structure on their mesophases and optical properties. The few studies of the flow behavior of SG-LCP melts have shown that the multiple levels of molecular and microscopic structure in SG-LCP systems give rise to rich rheological consequences.[2-4] Flow also provides a powerful means to manipulate molecular alignment in SG-LCPs.[4] To develop effective processing strategies for these materials, it is necessary to understand the effects of molecular structure on their steady and dynamic rheological behavior.

Some of the previous investigations of the viscoelastic behavior of side-group liquid-crystalline polymeric materials have produced intriguing results. Steady-shear experiments on SG-LCP melts revealed that, although the viscosity increased sharply at the nematic-to-smectic transition,[5] it remained continuous through the isotropic-to-nematic transition.[5,6] This indifference to the isotropic-to-nematic transition is surprising, since thermotropic main-chain LCPs,[7] small-molecule liquid crystals,[8] and lyotropic rigid-rod systems[9,10] show an abrupt drop in viscosity upon cooling from the isotropic to nematic state.

Two recent oscillatory shear studies of SG-LCPs led to apparently contradictory results. Using oscillatory shear, Colby et al.[3] reported that even the shape of the relaxation spectrum—the very signature of a viscoelastic material's dynamic response—is unaffected by the transition from the isotropic to the nematic phase. Their results are in accord with previous studies that concluded that the change from isotropic to nematic order does not affect the viscoelasticity of SG-LCPs. In contrast to previous researchers, Kannan et al.[2] found that the nematic and isotropic branches of the relaxation spectrum of an SG-LCP are distinct at low frequencies. They studied materials with much higher molar masses (20–150 times larger) than the SG-LCPs used in previous studies.[3,5,6] This suggests that molecular weight may influence the effect of the isotropic-to-nematic transition on the relaxation dynamics of SG-LCP melts. To determine the origin of this discrepancy with respect to previous studies, we characterize nematic SG-LCPs with molar masses that bridge the gap between those used in the two disparate groups of studies.

Another facet of SG-LCP melt rheology about which contradictory conclusions have been reported is whether or not macroscopic orientation of the director can be achieved by shearing nematic SG-LCPs. On the basis of the observation that the viscosity remained continuous through the isotropic-to-nematic transition, Zentel and Wu concluded that flow could not be used to macroscopically align nematic SG-LCPs.[5] In contrast, Kannan et al.[2] observed that shear not only induces alignment of the nematic phase but does so extremely rapidly relative to other means of producing the macroscopic alignment required for many of the proposed optical applications of SG-LCPs. Here, we probe the molecular-weight dependence of flow-induced alignment in nematic SG-LCP melts.

On the basis of the efficacy of flow in aligning other layered liquids,[11,12] we also examine the linear and nonlinear viscoelastic behavior of smectic SG-LPCs. We compare the behavior of the nematic and smectic phases, focusing on the interplay between molecular-weight and mesophase order in determining their flow behavior.

[⊗] Abstract published in *Advance ACS Abstracts,* April 1, 1995.

0024-9297/95/2228-3521$09.00/0

Table 1. Chemical Structure and Phase Transition Temperatures for SG-LCPs Used in This Study[a]

R	sample	M_w (10^{-3})	M_w/M_n	T_g (°C)	T_{sn} (°C)	T_{ni} (°C)
CH_3	PM6M-11	1130	1.54	46		115
	PM6M-3	312	1.34	41		113
C_4H_9	PM6B-32	3180	1.59	48	111	115
	PM6B-5	487	1.42	43	108	113

[a] R denotes the mesogen terminal group (see text). Molecular weights and polydispersities were measured by GPC. Transition temperatures were detected by DSC.

Experimental Section

Materials. The SG-LCPs used in this investigation have a methacrylate backbone, a hexamethylene spacer, and a 4-hydroxyphenyl benzoate mesogen terminated with either a methoxy (PM6M) or butoxy (PM6B) moiety. Molecular weights, polydispersities, and transition temperatures of these materials are summarized in Table 1. Multiple fractionation was used to achieve relatively low polydispersities. The synthesis and characterization of these samples are described elsewhere.[2]

Apparatus. Oscillatory shear experiments were performed in a Rheometrics RSA-II dynamic mechanical testing system. A shear-sandwich flow fixture was equipped with CaF_2 windows to permit observation during mechanical testing. The tool area was 2 cm^2. Gap thickness varied from sample to sample and ranged from 0.32 to 0.55 mm. The flow cell is described in more detail in a previous publication.[2]

Methods. Three types of oscillatory shear experiments were performed: (1) "frequency sweeps" using sufficiently low strain amplitude to probe linear dynamic response over up to 5 decades of applied frequency, (2) "single cycle" shearing experiments to determine the strain dependence of the dynamic moduli at a given frequency, and (3) "prolonged shearing" to manipulate the alignment of the liquid crystal using large-amplitude (40−110%) oscillatory shear at a fixed frequency for an extended period of time (hours).

To provide a reproducible initial condition, samples were heated well into the isotropic phase ($\approx T_{ni}$ + 10 °C) and held there for at least 20 min just before each set of shearing experiments to erase any previous strain history. To determine the effects of mesophase order and molar mass on SG-LCP relaxation dynamics, frequency sweeps were performed in the isotropic, nematic, and (if applicable) smectic phases of each sample. The response was taken to be within the linear viscoelastic regime when a 2−6-fold increase in the strain amplitude produced no discernible change in the dynamic moduli.

To determine the effect of prolonged shearing on SG-LCP relaxation dynamics, frequency sweeps were conducted at a fixed temperature within the nematic phase before and after prolonged large-amplitude shear. For the PM6B series, which exhibits both nematic and smectic-A phases, frequency sweeps in the smectic phase were coordinated with prolonged shearing experiments in two modes: (1) Frequency sweeps were conducted at a fixed temperature within the smectic phase before and after prolonged large-amplitude shearing at that temperature. (2) Frequency sweeps were performed at a single temperature within the smectic phase before and after subjecting the sample to prolonged large-amplitude oscillatory shear at a temperature in the *nematic* state.

Results

Linear Viscoelastic Response. The storage and loss moduli (G' and G'') of the four PM6M and PM6B polymers listed in Table 1 were measured at temperatures from 75 to 135 °C. Some data sets were omitted from Figures 1−5 for clarity.

Isotropic *vs* Nematic Phases. Within either the isotropic or nematic phase, all four SG-LCPs obeyed time−temperature ($t-T$) superposition. However, the isotropic and nematic phases have qualitatively different relaxation spectra for samples with sufficiently high molecular weights ($M_w \geq 1 \times 10^6$) (Figures 1 and 3), manifested by distinct curves in a Cole−Cole plot of G'' *vs* G'. The two families of curves converge at high modulus values. Therefore, the distinct isotropic- and nematic-phase master curves were shifted to superimpose at high frequency, corresponding to the high values of G' and G'' where the two families of curves converge on a Cole−Cole plot. Loss modulus master curves showed trends similar to storage modulus master curves (as is evident in Figure 1a,b) and therefore are not shown in Figures 2−6. A reference temperature of T_0 = 118 °C, in the isotropic phase for all materials, is used throughout this paper.

When shifted in this way, the dynamic moduli of all four SG-LCPs are indistinguishable at high reduced frequencies, ωa_T, above a critical value ω_c ($\omega_c' \approx 300$ rad/s, $\omega_c'' \approx 30$ rad/s), regardless of molecular weight, mesogen terminus, or phase (Figures 1−4). This commonality of the high-frequency relaxation signature is not surprising, since (1) the short-range internal (Rouse-like) modes probed by these quick oscillations should be independent of the length of the polymer chain and (2) the difference between methoxy and butoxy terminal moieties on the mesogen are unlikely to profoundly influence SG-LCP dynamics at the level of Rouse-like modes. In addition, this common portion of the relaxation spectrum indicates that the Rouse-like modes are insensitive to mesophase order (isotropic *vs* unaligned nematic).

The effects of liquid-crystalline order and molecular weight are manifested in the linear viscoelastic spectrum only at frequencies below ω_c' or ω_c''. For the higher molecular weight fractions of both PM6M and PM6B (Figures 1 and 3), the nematic branch falls below the isotropic branch at low frequencies ($\omega < \omega_c'$ or ω_c''). This behavior is consistent with that observed previously in an entangled PM6M ($M_w \approx 3 \times 10^6$), referred to here as PM6M-30.[2] A weak plateau emerges in the isotropic phase, and from the plateau modulus $G^0_{N,iso} \approx 1.2 \times 10^5$ dyn/cm^2 (estimated using the value of the storage modulus at the frequency where tan δ is at its minimum value[13]), we calculate an entanglement molecular weight of $M_{e,iso} \approx 2.7 \times 10^5$ in the isotropic phase. No plateau was observed for the lower molecular weight PM6M (Figure 2), consistent with its molecular weight ($M_w < 1.5M_{e,iso}$). In the nematic phase even the higher molecular weight material PM6M-11 has no plateau, making it impossible to determine the entanglement molecular weight of nematic PM6M.

Although the terminal loss modulus of PM6M-11 was not accessible over the temperature and frequency range of our measurements, based on the lowest frequency we could measure, we estimate a 2.6-fold drop in the zero-shear viscosity η_0 [$\eta_0 = \lim_{\omega\to 0} (G''/\omega)$] upon cooling through T_{ni}. While consistent with the behavior of small-molecule liquid crystals[8] and main-chain liquid-crystalline polymers,[7] this behavior contrasts with previous reports that showed no abrupt change in the viscosity of dynamic moduli of SG-LCPs at the onset of nematic liquid-crystallinity.[3,5]

For PM6B, the viscoelastic response of the higher molecular weight fraction showed a considerable plateau in the isotropic phase (Figure 3) of about $G^0_{N,iso} \approx 9.2 \times 10^4$ dyn/cm^2, corresponding to $M_{e,iso} \approx 3.5 \times 10^5$. Because only a slight plateau is discernible in the nematic phase, the value of $M_{e,nem}$ is more difficult to extract. To obtain a rough estimate of its value, we approximate $G^0_{N,nem}$ in two ways: (1) by the value of G'_{nem} at the same frequency used for the isotropic phase (i.e., $\omega a_T \approx 2$ rad/s), leading to $M_{e,nem} \approx 8 \times 10^5$

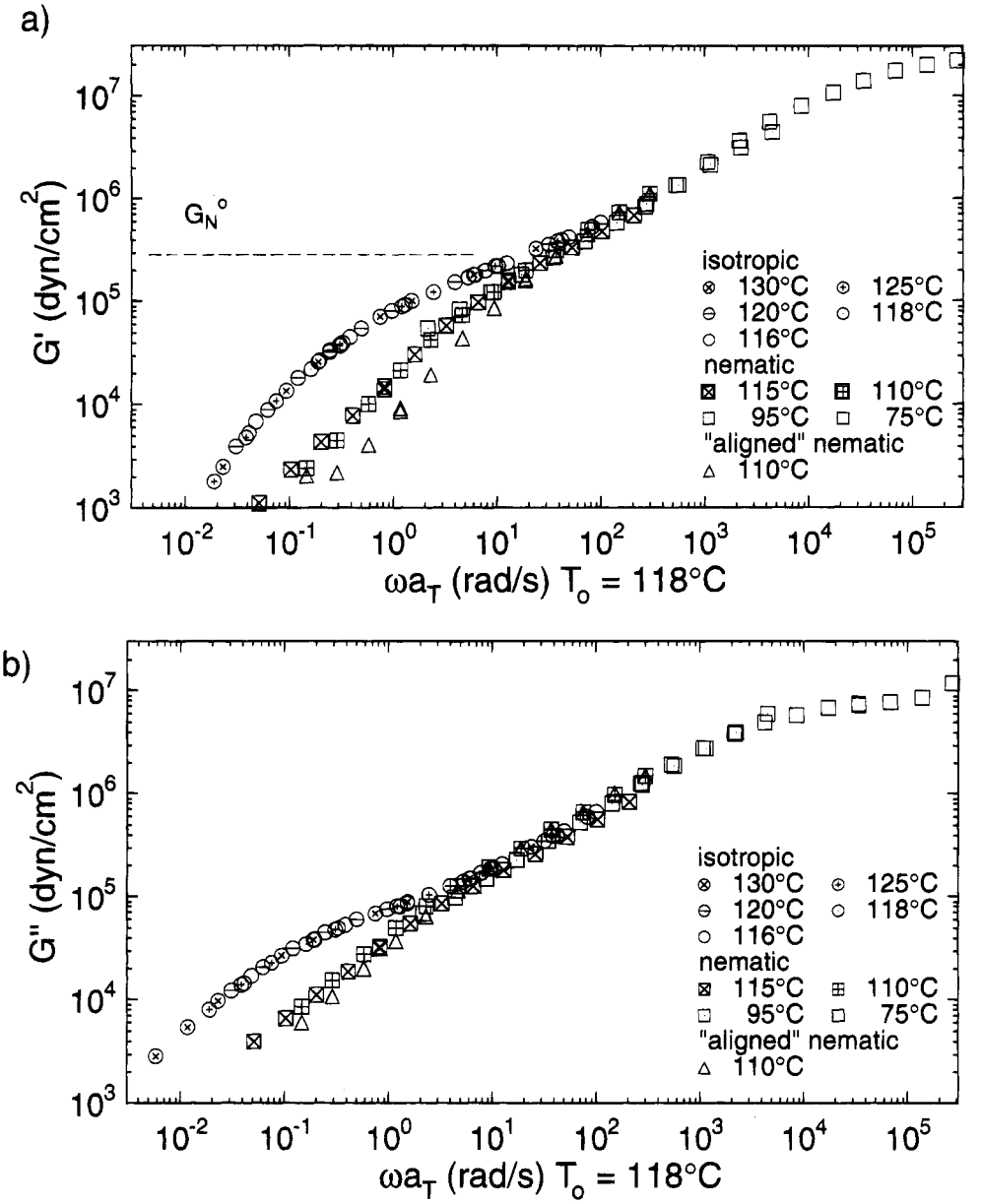

Figure 1. (a) Storage (G') and (b) loss modulus (G'') master curves [T_0 = 118 °C] for isotropic, nematic, and "aligned" nematic PM6M-11 [$M_w = 1.13 \times 10^6$]. Throughout this publication, all data gathered on a particular SG-LCP sample at a given temperature are horizontally shifted by the same amount, regardless of sample flow history. The term "aligned" refers to material that has been sheared to produce a transparent, highly birefringent nematic.

$\approx 2.3M_{e,iso}$, and (2) by the value of G'_{nem} at the minimum in tan δ_{nem} ($\omega a_T \approx 0.2$ rad/s), which gives $M_{e,nem} \approx 2.1 \times 10^6 \approx 6M_{e,iso}$. In either case, the rheological evidence (Figure 3) indicates that the polymer is less entangled in the nematic phase than it is in the isotropic phase. Possible explanations for this change in G^* at the isotropic–nematic transition are addressed in the Discussion section. In the smectic phase the plateau is dominated by the layered morphology rather than chain entanglements;[12] therefore, we cannot determine the effect of smectic order on entanglement based on the plateau modulus.

Smectic Phase. As in the nematic phase, the linear viscoelastic spectra of both molecular weight fractions of PM6B in the unaligned smectic state converge for $\omega \geq \omega_c$. Frequency sweeps in the smectic phase obeyed time–temperature superposition for both PM6B-32 and PM6B-5. As has been observed earlier in SG-LCPs,[3] main-chain LCPs,[14] and small-molecule liquid crystals[12] the storage and loss moduli of the smectic phase exceed those of either the nematic or isotropic phases and fail to reach terminal behavior even at the lowest accessible frequencies (Figures 5 and 6). It has recently been shown that such behavior is characteristic of unaligned layered liquids.[12]

Cole–Cole plots were examined to determine whether or not the smectic arm converges with the isotropic and nematic branches of the relaxation spectrum. This appears to occur, but at higher modulus levels (and correspondingly higher frequency) than the convergence of the isotropic and nematic branches. We use the overlap region of the Cole–Cole plot to identify the modulus range at which the smectic data should superpose with the nematic and isotropic data on a reduced frequency plot. The shift factors obtained show an abrupt jump at the nematic–smectic phase transition (Figure 7). For a given temperature, the shift factor determined for the unaligned smectic sample is applied to all data taken at that temperature, regardless of flow history (see below).

Temperature Dependence of Shift Factors. The temperature dependence of frequency shift factors for

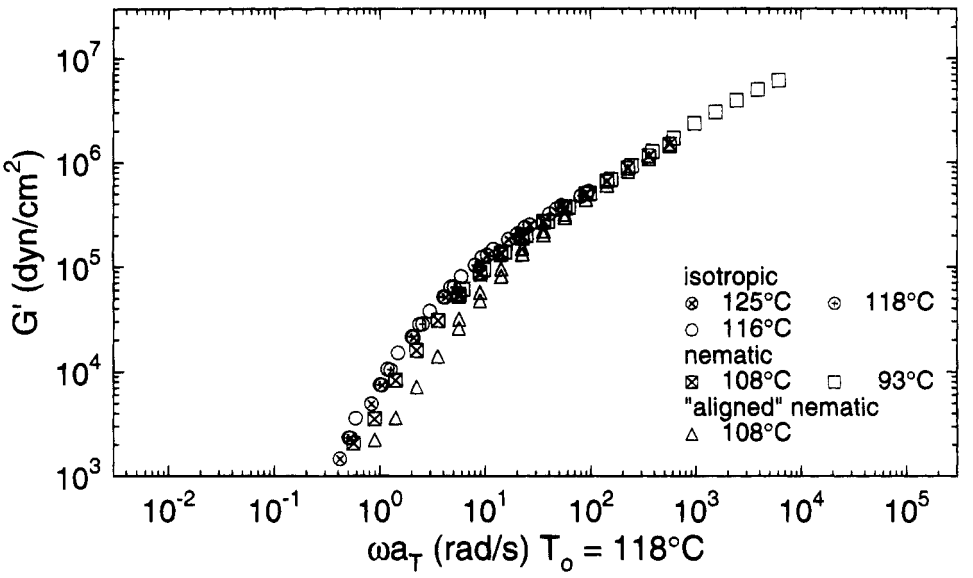

Figure 2. Storage modulus master curves [T_0 = 118 °C] for isotropic, nematic, and "aligned" nematic PM6M-3 [M_w = 3.12 × 10^5].

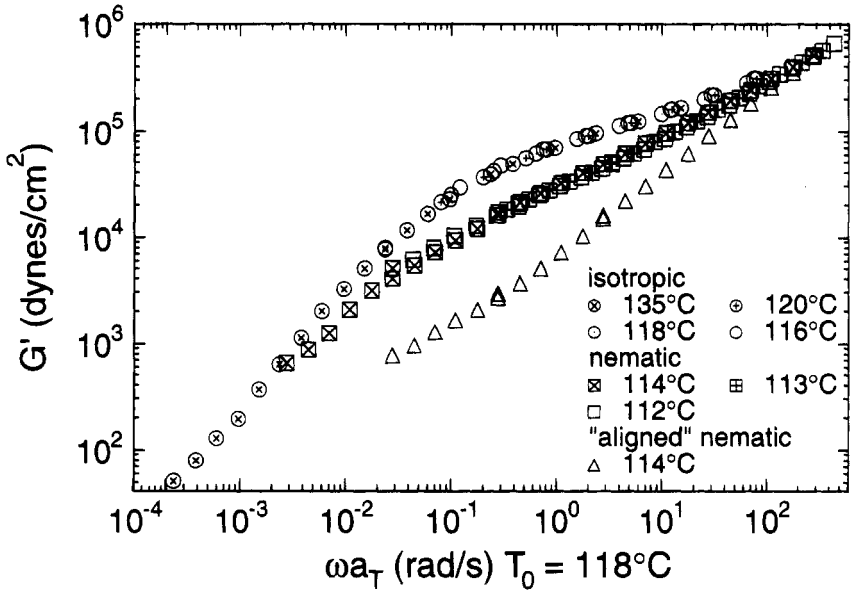

Figure 3. Storage modulus master curves [T_0 = 118 °C] for isotropic, nematic, and "aligned" nematic PM6B-32 [M_w = 3.18 × 10^6]. The high-frequency end of the viscoelastic spectrum can be seen more fully in Figure 5.

all fractions of PM6M and PM6B in the isotropic and smectic phases can be described by Arrhenius relationships, yielding apparent flow activation energies per backbone bond of 120 and 240 kJ/mol, respectively (Figure 7). The flow activation energies we observe in the isotropic and smectic phases are consistent with those reported earlier for lower-molar-mass PM6M and PM6B,[5] although the present values are somewhat higher (15–40%). In the nematic phase, the shift factors obey a WLF temperature dependence, with $\log a_T = [-C_1(T-T_0')/C_2+(T-T_0')]$, where the reference temperature T_0' is treated as an adjustable parameter and found to be T_0' = 396 K, with C_1 = 4.78 and C_2 = 108 K. The WLF behavior we observe in the nematic phase agrees well with the previously reported WLF dependence of the high-molar-mass PM6M-30[2] (Figure 7). Earlier studies have reported Arrhenius behavior for methacrylate-based nematic SG-LCPs with hexamethylene spacers,[3,5] including PM6M.[5] The Arrhenius activation energies of 159–175 kJ/mol, based on temperatures from 100–130 °C, reported in these two previous studies are in good agreement with the nematic-phase temperature dependence of the present samples over a comparable range in temperature.

Departure from Linear Response. In the isotropic phase, the effective dynamic moduli of PM6B-32 remain essentially independent of strain over the range of 0.1–100% and at ω = 100–0.1 rad/s. In the nematic phase, similar linearity is observed at high frequencies (≥10 rad/s). However, at lower frequencies (≤1 rad/s), strain *hardening* is observed at strains of 10% or more (Figure 8a). The strain dependence of G'' (not shown) is similar to that of G'. Indications of strain hardening in the nematic phase have been reported previously in PM6M.[4,15] The present results are in accord with the dynamic modulus of PM6M at ω = 0.1 rad/s and T = 110 °C reported both in the linear regime and in the first cycle of 100% strain used to induce alignment.[4,15] Qualitatively similar nonlinear behavior is observed in the nematic phase of PM6B-5 (Figure 8b).

In the smectic phase, PM6B is strain softening above $\gamma \approx 6\%$ for all frequencies at which the corresponding stress is measurable by our rheometer (Figure 9). This strain softening of the dynamic moduli in the smectic

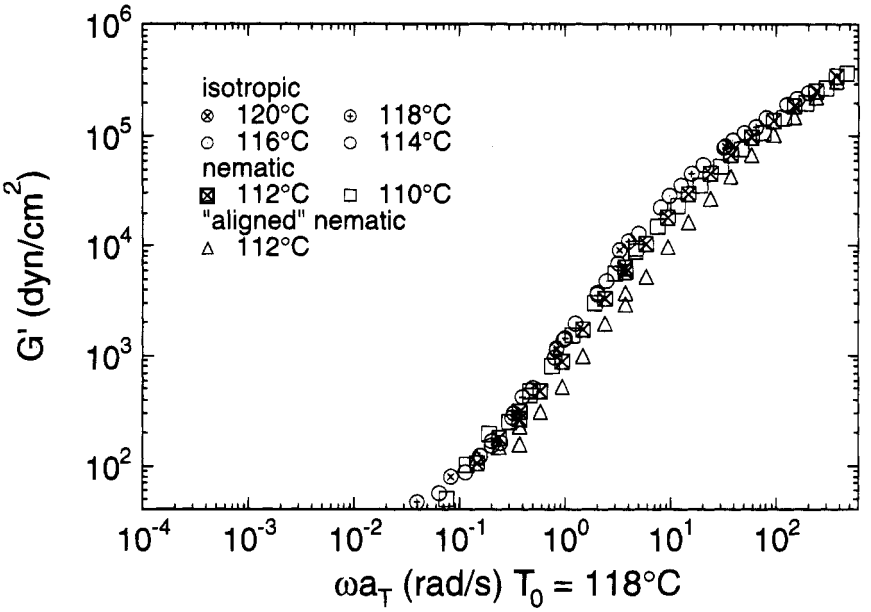

Figure 4. Storage modulus master curves [T_0 = 118 °C] for isotropic, nematic, and "aligned" nematic PM6B-5 [$M_w = 4.87 \times 10^5$]. The high-frequency end of the viscoelastic spectrum can be seen more fully in Figure 6.

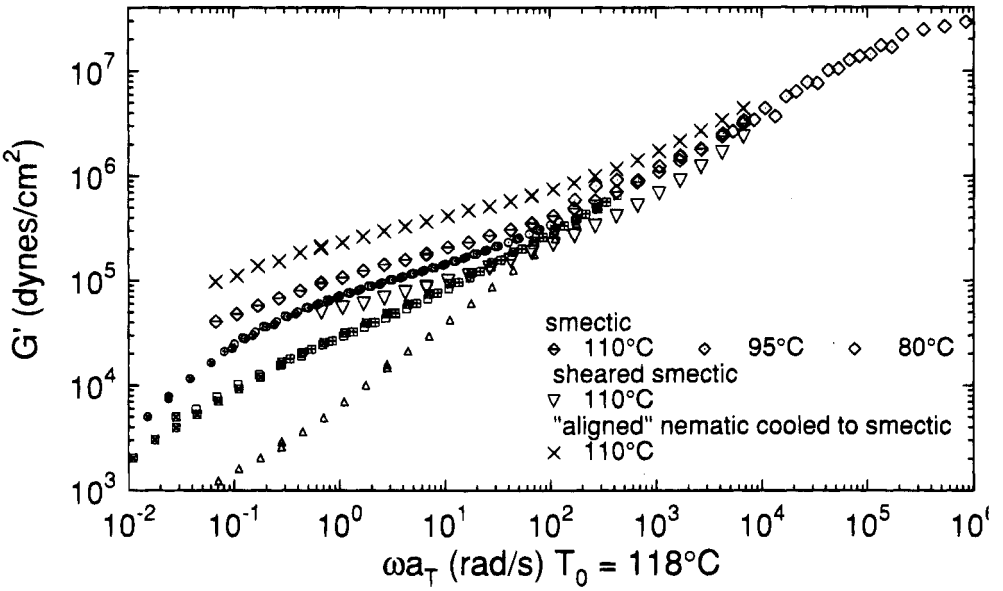

Figure 5. Storage modulus master curves [T_0 = 118 °C] for ordinary smectic and sheared smectic PM6B-32. Also shown are data from smectic PM6B-32 that has been shear-aligned in the nematic. Isotropic, nematic, and shear-aligned nematic data from Figure 3 are shown for comparison (small symbols).

phase is qualitatively similar to the behavior of another layered system, lamellar diblock copolymers.[16,17]

Consequences of Prolonged, Large-Amplitude Oscillatory Shear. Nematic Phase. Large-amplitude (100−110%) oscillatory deformations applied to polydomain nematic SG-LCPs cooled from an isotropic melt produced a dramatic change from an opaque, intensely scattering medium to a transparent and highly birefringent material.[4] As reported previously, this transformation was rapid, occurring within the first few cycles of shear. Shearing was continued for hundreds of cycles (typically 800). After cessation of large-amplitude shearing, the viscoelastic response of the material was probed with small-amplitude oscillations. The magnitudes of the low-frequency dynamic moduli ($\omega a_T < \omega_c$) of these shear-oriented materials were lower than those of the polydomain (unsheared) nematic (Figures 1−4), as had been observed earlier in PM6M-30.[2]

Although the rheological consequences of prolonged shearing were more pronounced for longer chains (*cf.* Figures 1a and 3 *vs* Figures 2 and 4), the effects of large-amplitude oscillatory shear on the turbidity and viscoelasticity of the nematic phase were observed for all samples studied, regardless of molecular weight or mesogen terminus. This demonstrates that, contrary to the conclusion reached by Zentel and Wu,[5] the linear viscoelastic response of the nematic phase need not be markedly different from that of the isotropic phase in order for flow to be an effective means of inducing macroscopic orientation.

Smectic Phase. Prior to the application of large-amplitude oscillatory shear, the smectic-phase polymer appeared an opaque white, indicating a high concentration of scattering defects. During sustained shearing, the polymer became slightly translucent but never attained the clarity or high birefringence characteristic of the shear-aligned nematic materials. Prolonged

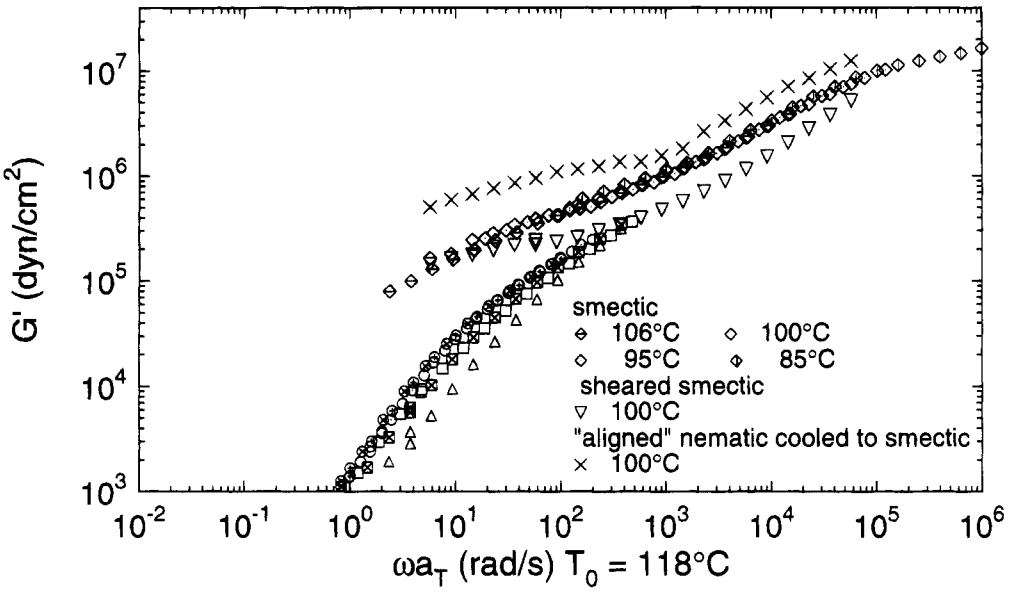

Figure 6. Storage modulus master curves [T_0 = 118 °C] for ordinary smectic and sheared smectic PM6B-5. Also shown are data from smectic PM6B-5 that has been shear-aligned in the nematic. Isotropic, nematic, and shear-aligned nematic data from Figure 4 are shown for comparison (small symbols).

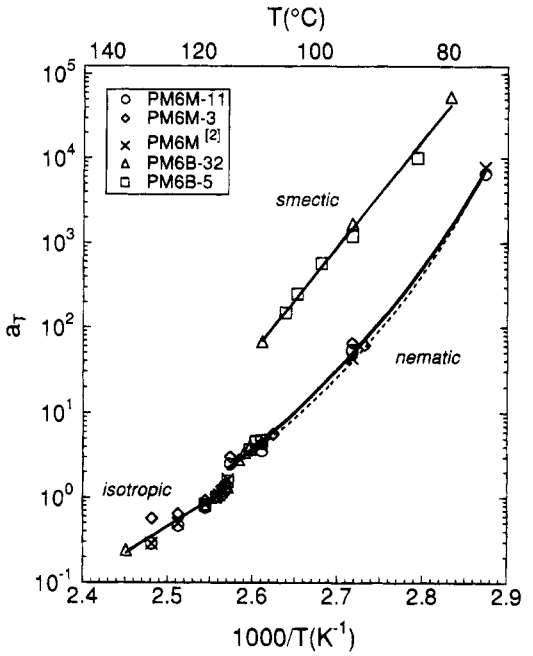

Figure 7. Temperature dependence of the shift factors (a_T) of PM6M and PM6B. Also shown for comparison are shift factors for PM6M-30 (×) and corresponding WLF dependence (dashed curve).[2]

large-amplitude oscillatory shearing (45% strain at 0.1 rad/s for 800 cycles at 110 °C) of smectic PM6B-32 did significantly reduce both the storage and loss moduli. Assuming that the procedure for time–temperature shifting the smectic phase frequency sweeps with respect to the nematic and isotropic data is correct, the shear-induced change in G' was not confined to frequencies below ω_c (Figures 5 and 6), suggesting that large-amplitude shearing induces profound structural changes in the smectic phase on length scales even shorter than those affected by shearing in the nematic phase.

Smectic SG-LCP Sheared in the Nematic Phase. After equilibrating at T_{ni} + 10 °C for 20 min to erase any prior strain history, PM6B-32 was cooled to the nematic state (T = 114 °C) and subjected to the identical large-amplitude shearing protocol described above (γ_0 = 45%, ω = 0.1 rad/s, 800 cycles). Upon cessation of shear, the aligned material was cooled into the smectic state (T = 110 °C) and allowed to equilibrate for 15 min. During this time the sample became progressively more turbid, suggesting the formation of defects. Nevertheless, the quenched smectic sample was still more translucent than the polydomain (unsheared) smectic material, which was completely opaque.

Immediately after temperature equilibration, the sample was probed with small-amplitude oscillatory shear. Surprisingly, the magnitudes of the resulting dynamic moduli *exceeded* those of the polydomain smectic polymer probed at the same temperature, frequency range, and strain amplitudes (Figure 5). The effects of previous large-amplitude oscillatory shearing in the nematic phase again manifested themselves in the smectic phase at shifted frequencies both above and below ω_c. In fact, even at frequencies some 1.5–2.5 decades higher than ω_c'' or ω_c', respectively, the effects of the shearing history are evident in the viscoelastic behavior of the smectic phase polymer. Qualitatively similar behavior was observed for the lower molecular-weight fraction of PM6B (Figure 6). This is significant in that ω_c represents a critical frequency above which oscillatory shear probes such local dynamics that the phase transitions alone have no impact on the relaxation spectrum.

Discussion

Entanglement Molecular Weight in the Isotropic Phase. The number of repeat units per entanglement (N_e) in isotropic PM6M and PM6B is very similar (Table 2), with somewhat higher N_e for the material with the bulkier side group.

The values of $N_{e,iso}$ are roughly on par with experimental values[18] for methacrylate polymers with large nonmesogenic side groups (Table 2). The group-contribution method of Wu overestimates the number of repeat units per entanglement strand of isotropic PM6M and PM6B by 30–35%.[19] The method of estimating M_e by Fetters et al.,[21] utilizing correlations between the plateau modulus, mean-square end-to-end distance, and density, leads to a value of $M_{e,iso}$ for PM6M within 5% of our experimentally-determined value of $M_{e,iso}$ = 2.7 × 10^5.

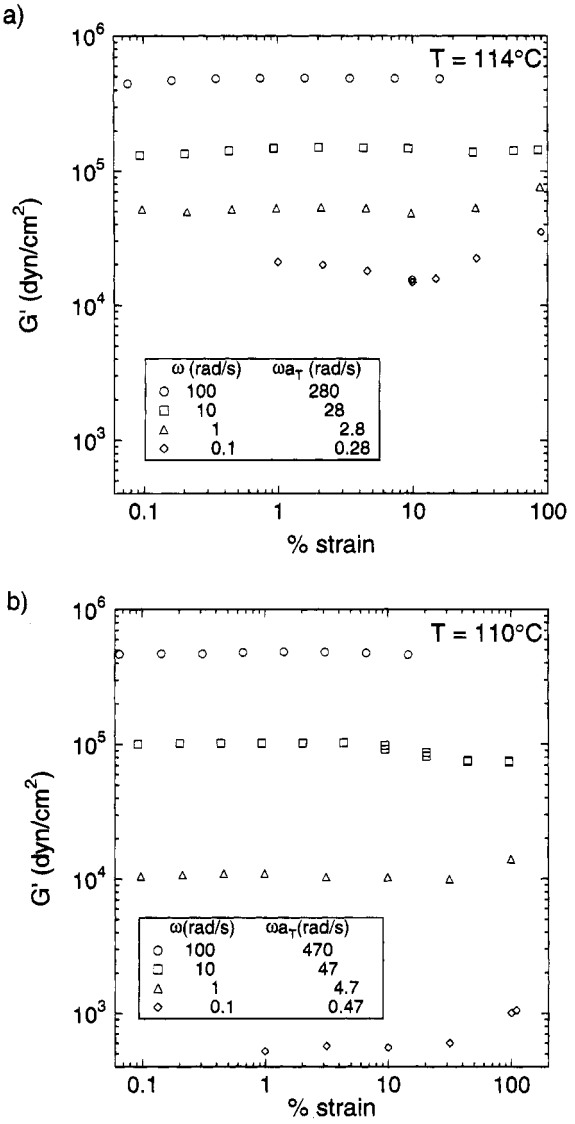

Figure 8. Strain dependence of the storage modulus (G') of (a) PM6B-32 (T = 114 °C) and (b) PM6B-5 (T = 110 °C) in the nematic phase.

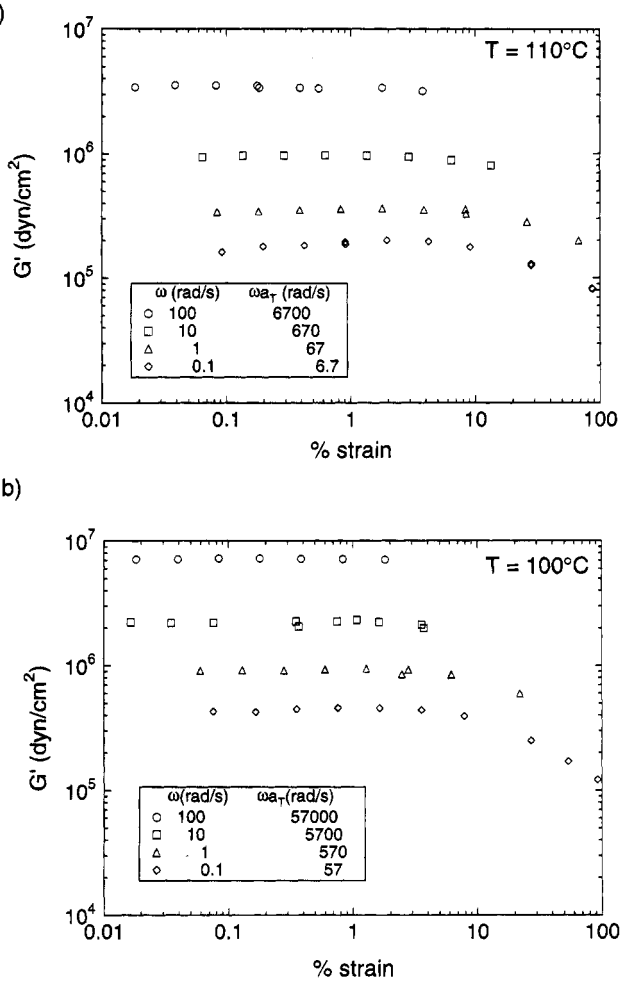

Figure 9. Strain dependence of the storage modulus (G') of (a) PM6B-32 (T = 110 °C) and (b) PM6B-5 (T = 100 °C) in the smectic phase.

Table 2. Number of Repeat Units per Entanglement Chain: Comparison of PM6M and PM6B with Other Polymethacrylates

methylacrylate polymer	M_e (10^{-3})	N_e
PM6B *isotropic*	**355**	**780**
PM6M *isotropic*	**270**	**660**
poly(triphenyl methacrylate)	203[19]	618
poly(4-*tert*-butylphenyl methacrylate)	69.7[19]	320
poly(diphenylmethyl methacrylate)	74.1[19]	278
poly(*n*-hexyl methacrylate)	33.8[18]	200
poly(*tert*-butyl methacrylate)	28.1[19]	198
poly(methyl methacrylate)	9.2[18]	92
	4.7[27]	47

The fact that the entanglement molecular weight of PM6M and PM6B in the isotropic phase is an order of magnitude larger than that of conventional poly(methyl methacrylate) discredits the recent assertion[20] that SG-LCP spacers behave as branches, increasing the entanglement density. Surprisingly, the chain contour length per entanglement appears to rise dramatically (by a factor between 2.3 and 6) upon cooling through the isotropic-to-nematic transition, as evidenced by a drop in the low-frequency modulus of the entangled materials (and an absence of any corresponding change in the relaxation dynamics of the unentangled polymer). This apparent increase in N_e in the nematic phase discredits the notion that the nematic mesogen field stabilizes entanglements.[20] Possible interpretations of the observed decrease in chain entanglement accompanying the isotropic-to-nematic phase change are addressed below.

Effect of Isotropic-to-Nematic Phase Transition. Comparison of the dynamic moduli of higher molecular weight versus lower molecular weight SG-LCP melts (Figures 1a and 3 *vs* Figures 2 and 4) clearly indicates that manifestation of nematic liquid crystallinity in the linear viscoelastic spectrum correlates with the emergence of a plateau in G' of the isotropic phase. We have considered various explanations for the molecular-weight-dependent drop in the dynamic modulus at the isotropic-to-nematic transition, such as (1) a decrease in the entanglement density due to an increase in the persistence length upon attaining nematic order; (2) a change in the friction coefficient of each repeat unit in the isotropic *vs* nematic melt; and (3) the possibility that "soft modes" in the nematic phase lead to energetically-favorable deformations, thus leading to lower moduli than in the isotropic phase. These alternatives are explored, and refuted, below. Finally, we are left with a working hypothesis involving a tube dilation that occurs without changes in contour length per unit volume but rather due to changes in the way polymer chains fluctuate among one another.

We consider the possibility that the constraints imposed by a locally-ordered mesogen field might effectively stiffen the chain, giving rise to a longer persistence length for the polymer backbone in the

nematic phase. On the basis of this assumption, one would expect to observe an expansion of the radius of gyration as the material is cooled through the isotropic–nematic transition. However, SANS experiments on PM6M and PM6B[22] reveal that, although the backbone assumes a slightly ellipsoidal rather than spherical shape in the nematic state, the overall mean dimension of the polymer coil remains essentially unchanged.

One might also argue that, with the onset of liquid-crystalline order, the viscosity experienced by the laterally attached mesogens might drop, as it does in small-molecule liquid crystals. This could produce a drop in the monomeric friction coefficient. However, this explanation can also be ruled out because such a decrease in resistance to chain movement should lead to an abrupt drop in the shift factor at the isotropic-to-nematic transition (in contrast to the rise observable in Figure 7), without any change in the shape of the viscoelastic spectrum, regardless of the degree of chain entanglement.

Another explanation for the difference in the moduli of the isotropic and nematic phases draws upon the balances in free energy of the mesogen field and the backbone. In side-group liquid-crystalline polymers, the backbone's propensity to assume a random-coil configuration is antagonistic to the mesogens' tendency to form an ordered microstructure. Although the flexible spacer serves to partially decouple these two opposing tendencies, orientational coupling between the backbone and mesogen still exists. It is possible that one consequence of the fact that the backbone spontaneously adopts an anisotropic conformation in the nematic phase might be that certain distortions of the chain are nearly iso-free-energy ("soft") deformations.[23] If the free energy cost of a given conformational distortion is higher when the pendant mesogens are isotropic than when they have nematic order, then the modulus in the isotropic phase might exceed that of the nematic polymer. However, the primary weakness in this interpretation is that it fails to address the molecular-weight dependence of the sensitivity of the linear viscoelastic spectrum to the isotropic–nematic phase transition (Figures 1–4). That is, this hypothesis would lead to a drop in modulus not only in the plateau region but also in the Rouse regime, contrary to what we observe. Furthermore, this hypothesis would lead to having a modulus that depends on the direction of mesogen alignment, in contradiction to recent results on magnetically-aligned nematic SG-LCP melts.[4]

Alternatively, we propose that the distinct viscoelastic behaviors exhibited by long SG-LCP chains in the nematic phase are related to an enhanced mobility of the mesogens in the nematic *vs* isotropic states. Experiments have shown that many low molar mass nematic liquid crystals exhibit faster diffusion in the mesophase than in the isotropic phase, with the diffusivities along ($D_{\parallel}$) and perpendicular to ($D_{\perp}$) the director having relative magnitudes $D_{\parallel} > D_{iso} \gtrsim D_{\perp}$.[25] In SG-LCPs, such enhanced mesogen mobility might permit larger lateral fluctuations of the polymer backbone to which mesogens are covalently tethered, as illustrated schematically in Figure 10. In the context of the reptation model, this corresponds to a dilation of the confining "tube" *without* an increase in R_g. Such tube dilation would be manifested by a decrease in the plateau modulus and terminal relaxation time of the entangled SG-LCP, consistent with the effect of nematic ordering on the dynamic moduli of PM6M-11 and PM6B-32 (Figures 1 and 3; Table 2). In particular, the increase in M_e of 2.3–6-fold suggested by our estimates

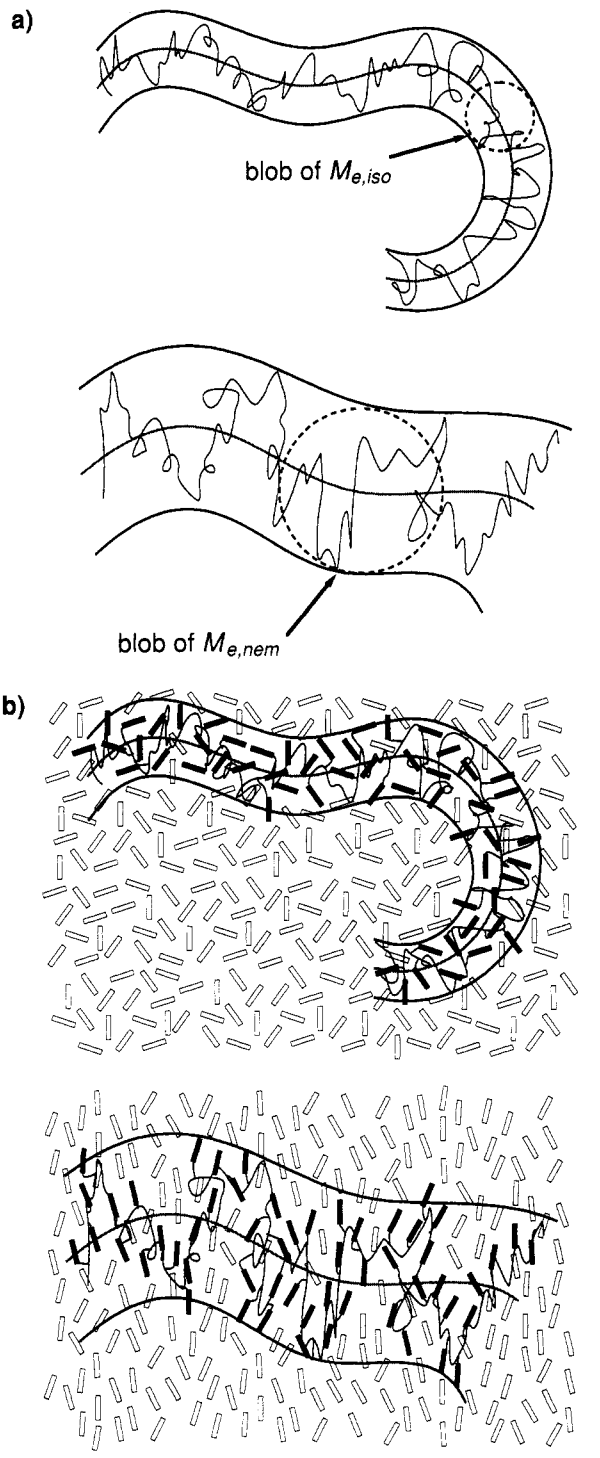

Figure 10. (a) Drop in the low-frequency modulus of entangled SG-LCPs at the isotropic-to-nematic transition which suggests a tube dilation associated with enhanced mesogen mobility. (b) As the material moves from the isotropic phase (top) to the nematic phase (bottom), the mesogens may offer less hinderance to lateral fluctuations. The effect is exaggerated in this schematic figure to illustrate the interpretation.

of $M_{e,nem}$ and $M_{e,iso}$ would correspond to a 1.5–2.4-fold increase in the tube diameter.

For nonentangled polymers (e.g., PM6M-3 and PM6B-5), lateral constraints imposed by neighboring chains do not limit conformational relaxation; therefore, increasing lateral freedom does not alter the shape of the relaxation spectrum, so the dynamic moduli are insensitive to the isotropic–nematic transition (Figures 2 and 4). We assume that the effective mobility of a Rouse segment chain is determined by the mean diffusivity, as is consistent with the observation that the isotropic–

nematic transition has little measurable impact on the monomeric friction coefficient (Figure 7).

This physical picture complements one suggested by Hall et al.[26] to explain tracer-diffusion data that seemed to indicate a strong *decrease* in the constraining tube diameter upon cooling from the isotropic to the nematic state for *main-chain* liquid-crystalline polymers. In this situation, the mesogenic unit is incorporated directly into the polymer backbone and therefore necessarily lies along the chain contour. Hence, the cage of surrounding mesogens in the nematic phase further confines movement transverse to the backbone relative to the isotropic phase. In contrast, the mesogens in PM6M and PM6B lie perpendicularly to the backbone; nematic order thus facilitates movement normal to the backbone contour.

To test the physical interpretation suggested above, one might investigate the molecular-weight dependence of the viscoelasticity of a SG-LCP whose mesogens tend to be *parallel* rather than *perpendicular* to their local backbone segment. In such a case, if the directional diffusivities indeed follow the order $D_{\parallel} > D_{\perp} \simeq D_{iso}$, one might expect the low-frequency relaxation dynamics of the nematic to differ comparatively less from the isotropic phase. Since phenyl benzoate mesogens with six-carbon spacers are known to have such a parallel coupling to an acrylate backbone,[22] the viscoelastic response of nematic and isotropic PA6M and PA6B should be characterized to see if the drop in modulus is absent in that system.

Strain Hardening in the Nematic Phase. The strain dependence of G^* in the isotropic and smectic phases is in accord with the behavior expected of amorphous melts and layered liquids, respectively. However, the nematic phase shows strain-hardening behavior which is not expected to arise from either the flexible backbone or the nematic liquid structure. This anomalous strain dependence at low frequencies and strains above 10% (Figures 8 and 9) may be due to the tendency of the mesogens to orient perpendicular to the backbone in the present SG-LCP, since the mesogens attached to a given strand may be forced to adopt an intermediate orientation between that dictated by the backbone segment and that dictated by the local orientation of the director.

This compromise (which may involve a reduction in the order parameter or a distortion of the spacer conformation or both) gives rise to a higher energy state for the local fluid structure. This increase in energy would be associated with an additional contribution to the modulus. If this contribution grows nonlinearly with strain, it could explain the observed strain-hardening behavior. A more detailed discussion of this mechanism for strain hardening and its relationship to a mechanism for flow-induced alignment of nematic SG-LCPs is given elsewhere.[4]

Effect of Shear History on the Smectic Phase. As has been found in other studies of the effect of shear on smectic phases, the modulus of the present SG-LCPs decreases when the smectic phase is subjected to shearing. Shearing does not produce a well-aligned material, also in accord with previous studies.[12] Surprisingly, we observe an *increase* in the dynamic modulus of the smectic phase produced by a history of shear in the nematic phase. The partial transparency of the smectic sample upon cooling from the aligned nematic state indicates a residual degree of alignment. A bias in the orientation distribution of the smectic could lead to the observed increase in the modulus, as has been established for other layered systems. In particular, when lamellae are oriented edge-on to the flow (layers tangent to the flow direction), lamellar block copolymers exhibit a lower modulus than the unaligned material; when the layers are broad-side to the flow (i.e., lamellae normal to the flow direction), the modulus is higher than that of the unaligned material.[11] If the smectic SG-LCP has a similar dependence of G^* on the orientation of the lamellae, then the increase in modulus would indicate that shearing in the nematic and cooling into the smectic leads to formation of layers biased such that the lamellae tend to lie normal to the direction of flow. However, the relationship between layer orientation and modulus in smectic SG-LCPs has not yet been established. Since the backbone in the smectic phase is in a highly distorted state ($R_{\parallel}:R_{\perp} \approx 4$),[22] its contribution to the modulus may be anisotropic. This could have the consequence that layers normal to the vorticity axis may have the highest modulus. To resolve these issues we must (1) determine the lamellar orientation distribution in a smectic obtained from a previously sheared nematic and (2) establish the effect of orientation on the dynamic modulus of smectic SG-LCPs.

A second possible explanation of the increase in modulus of the smectic phase obtained by cooling a shear-aligned nematic is that this flow and thermal history profoundly changes the microstructure of the smectic relative to the polydomain smectic SG-LCP. Instead of merely changing the orientation distribution of the layered structure, the process of heating to the nematic state, shearing, and requenching to the smectic phase may induce changes in the detailed organization of the fluid at the molecular level. Indeed, this is suggested by the fact that this treatment alters the relaxation signature of the smectic at *all* accessible frequencies.

Conclusions

By examining a series of PM6M fractions with molecular weights ranging from 3×10^5 to 3×10^6, we have determined that the effect of the isotropic-to-nematic transition on the flow behavior of the melt has a strong molecular-weight dependence. At high molecular weights ($M_w \geq 3 \times 10^5$), the dynamic moduli at low reduced frequencies are significantly lower in the nematic than in the isotropic state. For lower molecular weight samples the nematic and isotropic phases have virtually identical rheological behavior. Because rheological consequences of liquid crystallinity are observed only for entangled chains, we formulate a preliminary explanation within the context of the reptation model. We hypothesize that the decrease in plateau modulus indicates that nematic order increases the effective tube diameter relative to that in the isotropic phase; the enhanced mobility of the mesogens parallel to their long axis may lead to this increase in the amplitude of lateral fluctuations of the polymer backbone.

An unusual strain-hardening phenomenon is observed in the nematic phase of these SG-LCPs, which we attribute to a combination of (1) a strain-induced distortion of the polymer backbone which drives an energetically unfavorable disruption of the mesogen field and/or (2) nematic hinderance of the preferred perpendicular orientation between the backbone and mesogen, thus leading to energetically unfavorable relative orientations.

We find that flow-induced alignment of the nematic phase is possible for all the molecular weight fractions of the SG-LCPs used in this study. Contrary to assertions presented in the recent literature,[5] the linear viscoelastic response of the nematic phase need not be

markedly different from the isotropic phase in order for flow to be an effective means of producing aligned materials.

We find an appreciable drop in the modulus of the smectic phase after many cycles of large-amplitude oscillatory shear; however, the sample remains turbid throughout the shearing process, indicating that a high density of defects remains. A smectic material heated into the nematic phase, shear-aligned, and cooled to the smectic phase shows an *increase* in modulus. We have put forth two possible explanations: one hypothesis attributes the sample's increased modulus to a change in the orientation distribution of the smectic layers; the second attributes the increase in modulus to a change in the local organization of the fluid structure in the smectic SG-LCP melt. To discriminate between possible explanations of this phenomenon, experiments are underway to determine both the lamellar orientation and backbone conformation in sheared smectic SG-LCPs and to characterize the effect of lamellar orientation on the dynamic moduli of smectic SG-LCPs.

Acknowledgment. The authors thank U. Pawelzik for synthesizing and characterizing PM6M and PM6B. We gratefully acknowledge financial support from the National Science Foundation Presidential Young Investigator Award (J.A.K.) and Graduate Fellowship (S.F.R.) programs, the Gates–Grubstake Fund, the Caltech Consortium for Chemistry and Chemical Engineering (E.I. duPont de Nemours and Company, Inc., and Eastman Kodak Company), and the NATO-Travel Grant Program (CRG 001037).

References and Notes

(1) McArdle, C. M., Ed. *Side Chain Liquid Crystal Polymers*; Chapman and Hall: New York, 1989.
(2) Kannan, R. M.; Kornfield, J. A.; Schwenk, N.; Boeffel, C. *Macromolecules* **1993**, *26*, 2050.
(3) Colby, R. H.; Gillmore, J. R.; Galli, G.; Laus, M.; Ober, C. K.; Hall, E. *Liq. Cryst.* **1993**, *13*, 233.
(4) Kannan, R. M.; Rubin, S. F.; Kornfield, J. A.; Boeffel, C. *J. Rheol.* **1994**, *38*, 1609.
(5) Zentel, R.; Wu, J. *Makromol. Chem.* **1986**, *187*, 1727.
(6) Fabre, P.; Veyssie, M. *Mol. Cryst. Liq. Cryst. Lett.* **1987**, *4*, 99.
(7) Wissbrun, K. F.; Griffin, A. C. *J. Polym. Sci., Polym. Phys. Ed.* **1982**, *20*, 1835.
(8) Porter, R. S.; Johnson, J. F. *Rheology*; Eirich, F. R., Ed.; Academic Press: New York, 1967.
(9) Baird, D. G. *Liquid Crystalline Order in Polymers*; Blumstein, A., Ed.; Academic Press: New York, 1978.
(10) Papkov, S. P.; Kulichikhin, V. G. *J. Polym. Sci., Polym. Phys. Ed.* **1974**, *12*, 1753.
(11) Koppi, K. A.; Tirrell, M.; Bates, F. S.; Almdal, K.; Colby, R. H. *J. Phys. II (Fr.)* **1992**, *2*, 1941.
(12) Larson, R. G.; Winey, K. I.; Patel, S. S.; Bruinsma, R. *Rheol. Acta* **1993**, *32*, 245.
(13) Wu, S. *J. Polym. Sci., Polym. Phys. Ed.* **1987**, *25*, 2511.
(14) Hudson, S. D.; Lovinger, A. J.; Larson, R. G.; Davis, D. D.; Garay, R. O.; Fujishiro, K. *Macromolecules* **1993**, *26*, 5643.
(15) Kannan, R. M.; Kornfield, J. A.; Schwenk, N.; Boeffel, C. *Adv. Mater.* **1994**, *6*, 214.
(16) Rosedale, J. H.; Bates, F. S. *Macromolecules* **1990**, *23*, 2329.
(17) Winey, K. I.; Patel, S. S.; Larson, R. G.; Watanabe, H. *Macromolecules* **1993**, *26*, 2542.
(18) Wu, S. *J. Polym. Sci., Part B: Polym. Phys.* **1989**, *27*, 723.
(19) Wu, S. *Polym. Eng. Sci.* **1992**, *32*, 823.
(20) Götz, S.; Stille, W.; Strobl, G. *Macromolecules* **1993**, *26*, 1520.
(21) Fetters, L. J.; Lohse, D. J.; Richter, D.; Witten, T. A.; Zirkel, A. *Macromolecules* **1994**, *27*, 4639.
(22) Kirste, R. G.; Ohm, H. G. *Makromol. Chem., Rapid Commun.* **1985**, *6*, 179.
(23) Warner, M.; Bladon, P.; Terentjev, E. M. *J. Phys. II (Fr.)* **1994**, *4*, 93.
(24) Doi, M.; Edwards, S. F. *The Theory of Polymer Dynamics;* Oxford University Press: New York, 1986.
(25) Krüger, G. J.; Spiesecke, H., Van Steenwinkel, R.; Noack, F. *Mol. Cryst. Liq. Cryst.* **1977**, *40*, 103.
(26) Hall, E.; Ober, C. K.; Kramer, E. J.; Colby, R. H.; Gillmor, J. R. *Macromolecules* **1993**, *26*, 3764.
(27) Ferry, J. D. *Viscoelastic Properties of Polymers*, 3rd ed.; Wiley: New York, 1980.

MA941248+